www.sciencemag.org/cgi/content/full/science.1258750/DC1

Supplementary Materials for

Semiaquatic Adaptations in a Giant Predatory Dinosaur

Nizar Ibrahim,* Paul C. Sereno, Cristiano Dal Sasso, Simone Maganuco, Matteo Fabbri, David M. Martill, Samir Zouhri, Nathan Myhrvold, Dawid A. Iurino

*Corresponding author. E-mail: nibrahim@uchicago.edu

Published 11 September 2014 on *Science* Express
DOI: 10.1126/science.1258750

This PDF file includes:

Supplementary Text

1. New Fossil Material

    New Partial Skeleton

    New Referred Specimens

2. Taxonomy of *Spinosaurus aegyptiacus* Stromer 1915

    Neotype Designation

    Taxonomic Diagnosis

    Referred Material, Junior Synonym

---

1. New Fossil Material

New Partial Skeleton

The neotype (FSAC-KK 11888) consists of a partial subadult skeleton including fragmentary remains of the skull and portions of the axial column, manus, pelvic girdle, and hind limbs. Preserved cranial bones include portions of the nasal, prefrontal, squamosal, quadratojugal, most of both quadrates, dentary sections, isolated teeth and a

possible lacrimal. Axial bones include partial cervical, dorsal, sacral, and caudal vertebrae, partial cervical and dorsal ribs, and partial chevrons. The forelimb is represented by manual digit II-2 phalanx and the base of phalanx 3. Both sides of the pelvic girdle and hind limbs are well represented (femora, tibiae, fibulae, pedal phalanges, ilia, ischia, pubes). A nearly complete pes is preserved (fig. S1), although no part of the ankle is preserved.

New Referred Specimens

Many specimens have been referred to *Spinosaurus aegyptiacus* based on overlap or similarity of the bones to those originally described by Stromer (*5, 11*).

The neotype specimen is going to be housed at the FSAC (Casablanca). New isolated specimens of *S. aegyptiacus* included here are housed in the University of Chicago Research Collection:

UCRC PV4	Left dentary mid section with roots lacking crowns (subadult).
UCRC PV5	Mid caudal vertebra.
UCRC PV6	Distal caudal vertebra.
UCRC PV7	Distal caudal vertebra.
UCRC PV8	Left digit I-1 manual phalanx.

Nasals with a fluted crest referred to *Spinosaurus* and housed in the UCRC were described in the past (*6*).

Specimens housed at the Museo di Storia Naturale di Milano in Italy include:

MSNM V4047	Complete snout and rostrum (*6*)
MSNM V6353	Pedal phalanx III-1
MSNM V6849	Distal caudal vertebra
MSNM V6872	Anterior dorsal vertebra (D3–D4)
MSNM V6874	Cervicodorsal vertebra (C10–D1)
MSNM V6877	Cervicodorsal vertebra (C10–D1)
MSNM V6881	Anterior dorsal vertebra (D2)
MSNM V6886	Proximal manual phalanx
MSNM V6888	Pedal phalanx
MSNM V6893	Right metacarpal III
MSNM V6896	Left quadrate (subadult)
MSNM V6897	Pedal phalanx
MSNM V6900	Left ilium (subadult)
MSNM V7142	Metatarsal, distal portion
MSNM V7143	Anterior dorsal vertebra (D1–D2)

We also refer a large humerus (NMC 41852), described and figured by Russell (1996) as an indeterminate theropod specimen to *Spinosaurus*. As noted by Russell (1996), it differs from humeri of other theropods, and appears to be surpassed in size only by the humeri of *Therizinosaurus* and *Deinocheirus*. It is unlikely that NMC 41852 belongs to one of the other Kem Kem theropods. In *Deltadromeus* the humerus is more slender and

elongate (*7*). The humeri in allosauroids (such as *Carcharodontosaurus*) are proportionally much shorter, as are those of ceratosaurs. It is noteworthy that NMC 41852, which is missing the distal and proximal ends, compares quite favourably with the humerus of *Baryonyx*, the only notable difference being that the humeral shaft is more elongate in the former. The widely expanding distal margin however, suggests a similar outline to that of *Baryonyx*. Furthermore, the height of the deltopectoral crest and the internal tuberosity is the same in both specimens. The proximal end also appears to be expanding posteriorly in a similar way. Increasing the humerus of *Baryonyx* to about twice its size (several cranial remains of *Spinosaurus* are about twice the size of corresponding elements in *Baryonyx*), renders it similar in size and morphology to NMC 41852. That *Spinosaurus* is a very large theropod, and very likely the longest theropod in the Kem Kem by a considerable margin further adds to the likelihood of this identification. Considering that no evidence exists for an as yet unknown very large taxon with a giant humerus, it is most parsimonious to refer this specimen to *Spinosaurus* in the light of the noticeable morphological similarities with *Baryonyx*. We propose that the giant humerus NMC41852 is referable to *Spinosaurus.* Similarly, an isolated ulna (FSAC-KK 11889), collected at Aferdou N'Chaft in the Kem Kem region, matches the shape of the ulna in *Suchomimus* remarkably well, with the exception that, like the humerus described above, it has a more flattened profile. We also refer this specimen to *Spinosaurus*. Large isolated claws from the Kem Kem (*11*) match the elongate morphology of the manual elements and are here also referred to *Spinosaurus*.

2. Taxonomy of *Spinosaurus aegyptiacus* Stromer 1915

Neotype Designation

Associated remains of *Spinosaurus aegyptiacus* are extremely rare. A century has passed since the discovery of two associated specimens in Egypt and over 70 years have passed since these remains were destroyed in a bombing raid in WWII (*3*, *4*). Recent excavation of a partial subadult skeleton that preserves portions of the skull and postcranial skeleton provides a long-awaited opportunity to designate a neotype for *S. aegyptiacus*. The find was made by a local collector in 2008, when one of us (NI) was leading field work in the Kem Kem beds. The initial portion of the specimen was tentatively identified at that time as *Spinosaurus* by NI and SZ and acquired by the University of Casablanca (FSAC). When additional elements of the specimen came to light in Milan in 2009, CDS and SM involved NI. Subsequently, the collector was relocated, and he took three of us (NI, DMM, SZ) to the excavation site. In 2013, complete excavation of the site by NI, PCS, CDS, DMM, SZ and colleagues resulted in the recovery of many additional pieces belonging to the neotype.

In designating this specimen as a neotype, we follow the guidelines set forth in Article 75.3 of the International Commission on Zoological Nomenclature, which states that there needs to be:

- an exceptional need;
- a distinctive taxon;
- details allowing recognition of the specimen;
- reasons why it is believed the name bearing types are destroyed;

- evidence that the neotype is consistent with what is known of the former name bearing types;
- evidence that the neotype came from as close as practicable to the original type locality;
- a statement that the neotype is, or has become, the property of an institution which can preserve it and make it available for study.

There is sustained interest and research on the early Late Cretaceous vertebrate faunas of North Africa. Sorting out the morphology and taxonomy of the predatory dinosaurs is a key component of understanding this time period, its vertebrate diversity, paleoecology and relationship with faunas on adjacent landmasses. *S. aegyptiacus* is a unique theropod in several important aspects and will likely remain a taxon of intense interest for its size, adaptations, and life habits. There is no question that the holotype and referred fossils from Egypt collected by Stromer have been destroyed. Return expeditions to Stromer's localities in Egypt have failed to discover substantial additional material of *S. aegyptiacus* (*4*). Rather, the best new fossils of this species have been discovered in Algeria and the coeval Kem Kem beds of Morocco (*5*, *6*).

The neotype specimen can be referred to *S. aegyptiacus* based on the very similar form of the dorsal vertebrae, including the long, pinched hour-glass shaped centra and the hypertrophied neural spine with its flared base, narrow mid-section and surficial striations. The neotype is catalogued in the collections of the Faculté des Sciences Aïn Chock in Université Hassan II in Casablanca, Morocco, where it will reside by the end of 2014.

Taxonomic Diagnosis

We provide a diagnosis below for the genus *Spinosaurus*, which also will serve as the diagnosis for its sole valid species, *S. aegyptiacus*. As was common tradition at the turn of the century, Stromer (*1*) did not properly diagnose the genus and species by today's standards. After describing the initial specimens, he named the genus and species, mentioning only one feature that might stand as an autapomorphy—the elongate dorsal neural spines. Despite strong interest in *S. aegyptiacus*, the taxon has yet to receive an adequate taxonomic diagnosis.

SPINOSAURIDAE Stromer, 1915

Sigilmassasauridae Russell, 1996

SPINOSAURINAE Stromer, 1915

SPINOSAURUS Stromer, 1915

Sigilmassasaurus Russell, 1996

SPINOSAURUS AEGYPTIACUS Stromer, 1915

Sigilmassasaurus brevicollis Russell, 1996

Spinosaurus maroccanus Russell, 1996

Neotype: FSAC-KK 11888, partial skeleton including bones from the skull, axial column, forelimb, pelvic girdle and hind limb (see list above, figs. S2, S3).

Locality and Horizon: Zrigat, southeastern Morocco; 31° 37’ N, 4° 16’ W.

Emended Diagnosis: Spinosaurid with adult body length ~15 m characterized by the following cranial features: external naris and narial fossa small and retracted near the orbit on the side of the posterior snout; premaxilla excluded from the border of the external naris. Distinguishing postcranial features include strongly constricted hourglass-shaped and elongated dorsal centra; dorsal neural spine height up to ten times greater than centrum height; greatest anteroposterior dorsal neural spine width below spine apex; dorsal neural spines composed of dense bone with a narrow central zone of cancellous bone; proximal one-third of dorsal neural spines textured externally by vertical striae; long bones lack open medullary cavity; length of ilium larger than dorsoventral length of femur; femur strongly bowed anteriorly with fourth trochanter hypertrophied, extending along ~25% of the femoral shaft; pedal digit I long, digit I-1 phalanx longest nonungual phalanx in the pes; pedal unguals broader than deep with length almost four times proximal depth; pedal unguals with flat ventral surface.

Referred Material, Junior Synonym

Although hundreds of isolated bones and teeth of *S. aegyptiacus* are in collections around the world, a few specimens are more complete and thus have garnered attention. **“***Spinosaurus* B”. Stromer designated bones found in close association as “*Spinosaurus* B” (*2*), a partial skeleton that was entirely destroyed in WWII. The unusual proportions of the neotype (reduced pelvis size and short hind limb length compared to the axial

column) are also present (and nearly identical) in this specimen (fig. S2), suggesting that it composed a second associated individual of *S. aegyptiacus*.

Spinosaurus maroccanus. This species was based on a single supposed proportional difference using measurements given by Stromer (*11*). We regard this difference as an artifact of differing ways to measure opisthocoelous vertebrae. Following the conclusions of previous studies (*6*, *13*). We regard this species as a *nomen dubium*.

Sigilmassasaurus brevicollis. We examined fossils of *Sigilmassasaurus brevicollis*, which we regard as a junior symonym of *Spinosaurus aegyptiacus*. One or more of the characteristic cervicodorsal vertebrae attributed to this taxon are now known in associated specimens in several spinosaurids including "*Spinosaurus* B" and probably *Baryonyx* and *Suchomimus*. In the latter two genera, the cervicodorsal vertebrae of interest are somewhat fragmented (*Baryonyx*) or not completely exposed (*Suchomimus*), although both seem to show many of the suite of features that characterize these cervicodorsal vertebrae. These include a very low and broad centrum, strong opisthocoely, small pleurocoels, a prominent ventral keel, strong transverse processes, and broad zygapophyseal facets with very low epipophyses. There is no justification for the differentiation of this taxon from *S. aegyptiacus.*

3. Skeletal Measurements

Principal measurements of the neotype skeleton and comparisons with other theropods are given in Tables S1 and S2.

4. CT-Scanning and Digital Reconstruction

A multicolored digital skeletal model (fig. S3) shows the origin of bone information and some of the inferences that were made. There is some overlap between specimens pertaining to *S. aegyptyiacus*. When this occurs, precedence in the color model is given in the order in which the colors are listed in the figure: neotype, Stromer's bones, isolated bones, surrogate bones, and inferred bones.

The cheek region of the skull (including the jugal and postorbital), the braincase, the palatal bones, and the surangular and bones on the medial aspect of the lower jaw remain unknown in *S. aegyptiacus* (fig. S4). Most of these bones, however, are known in other spinosaurids.

CT-Scanning

A Philips Brilliance iCT 256-slice multi-detector CT scanner was used to scan the specimens at the University of Chicago Medical Center. A kVp of 120-140 was used for most specimens, depending on size and density. A mAs of 175 (without dose modulation) generated the best results with a Philips YC filter (high resolution, sharp and noisy) and slice thickness of 0.67 mm. Each scan was reconstructed using Materialise Mimics v. 16.0 and individual bones were exported as .stl files. They were then imported into ZBrush to reconstruct missing pieces or as references for missing bones.

Flesh Rendering

The digital *Spinosaurus* skeleton was wrapped for flesh rendering as follows. The skeleton was positioned in a 'neutral' pose and opened in the digital sculpting program

ZBrush (Pixologic, Inc.). A spherical 3D mesh called "Sphere3D" was placed within the ribcage of the skeleton, and the Move, Standard, and Smooth brushes were used to stretch it from snout tip to tail tip, pulling so that it covered the underlying bones of the axial skeleton. Then a 3D mesh ("ZSphere") was placed both at the sagittal plane of the pelvis and at the sagittal plane of the pectoral girdle. Each ZSphere created a base mesh that could be pulled out along the limb bones, including the manual and pedal phalanges. The meshes were merged into a single mesh and Dynameshed to create a uniform distribution of polygons across the surface.

Using the extant phylogenetic bracket with reference to crocodilians and birds, landmarks for muscle attachment were noted and the mesh was further sculpted to approximate the limb and tail muscles. The Transform: Transparent button could be toggled on and off to evaluate the soft tissue mesh in relation to the skeleton within. Variations of soft tissue thickness were easily generated by editing the mesh. The skin mesh was saved as .stl files and exported for center of mass estimation.

Center of Mass Estimation

Center of Mass was estimated using Meshlab. Within Meshlab the model was processed as follows: Filters > Quality Measures and Computations > Compute Geometric Orders. This creates an output including Mesh Bounding box, MeshVolume, and Center of Mass. Using this output with Render > Show Quoted Box, the center of mass via X, Y, Z coordinates can be plotted. For more information see (*31*).

5. Maturation and Bone Density Profile

Ontogenetic Status of the Neotypic Skeleton

The age and maturity of the neotypic specimen can be inferred from its relative size, growth indicators and analysis of histological thin-sections. By comparing the preserved cranial and postcranial bones with the largest specimens referred to *S. aegyptiacus*, the neotype specimen can be shown to be a subadult individual approximately 32% smaller than maximum adult size across a range of measurements. Neurocentral sutures preserved in the vertebrae do not exhibit coossification, nor is there coossification between sacral centra or between the ilium and sacral vertebrae.

Two long bones (femur, fibula), a possible gastralium and the proximal end of a dorsal rib were selected for histological thin sections. The thin-section of the femur is composed of fibrolamellar bone that becomes increasingly cancellous towards the center. Vascularization is prevalently reticular. The composite structure of the bone is a reticular fibrolamellar bone. Vascular canals are still open, even if infilling of lamellar bone is present. Vascularization tends to decrease towards the surface, even if still present in the outer cortex. Haversian systems are present and dominant in the inner cortex, covering two-thirds of the primary bone.

We estimate that six to seven years of growth are represented in the primary cortex. We performed a retrocalculation to assess the number of zones obscured from remodeling. The major and minor axes of the bone's cross-section were identified with ImageJ (*32*). For a consistent count of missing lines of arrested growth (LAG), we employed three recognition criteria: the broadest zone, taken as representative of each missing band; the ultimate or penultimate zone; the mean interval between the three

innermost zones. Using each criterion, respectively, we calculated 8.35, 13.1 and 13.67 missing LAGs, with a resulting mean of 11-12 years missing. Thus we estimate the age of the neotype at the time of death is ~17 ± 2 years.

An external fundamental system is not found in any of the four bones sectioned, and vascularization is still present in the circumferential layer. We infer a subadult ontogenetic stage for the neotypic specimen. This interpretation is also based on the high amount of Haversian systems in the inner cortex, the decrease in density of vascularization towards the surface of the cross section and the decrease in spacing between LAGs towards the outer cortex. Maximum adult size would likely have entailed many years of subsequent growth.

Bone Density

We compared bone compactness in femoral shaft thin-sections in *S. aegyptiacus* (Table S3) and *Suchomimus tenerensis*, in other nonavian, and in avian theropods, some of which are shown in phylogenetic context here (fig. S5). Values of compactness for extant taxa were taken from Quemeneur et al. (*34*); images of the thin-sections are from the literature. One exception is *Tyrannosaurus rex*, because the only thin-section published pertained to the tibia. The thin-sections were drawn and colored in black and white. The values taken into account in our comparison are S, P, Global Compactness, Compactness at the center, Compactness in the periphery, and the Compactness Profile (*23*).
The values of compactness of *S. aegyptiacus* are comparable with the values of *Aptenodytes patagonicus* (king penguin) and higher than values for *Alligator mississippiensis* (Table S4). *Suchomimus tenerensis* shows values of compactness closer

to other theropods and extant terrestrial taxa. The presence of hollow shafts in theropod long bones is a very common feature even in basal members, such as *Herrerasaurus* and *Eodromaeus* (*42*, *43*).

The lack of an open medullary cavity and increase in density cannot be explained as an ontogenetic artifact. Taphonomic factors also cannot account for the high-density value for *S. aegyptiacus*, because a femoral section of another theropod from the same deposit ('Kem Kem theropod') shows an open medullary cavity and lower density. There seems to be no correlation between body size and compactness: *Tyrannosaurus* and *Allosaurus* show lower compactness than a penguin (*Aptenodytes patagonicus*) or extinct birds (*Ichthyornis*, *Hesperornis)* with a semiaquatic lifestyle. High compactness is found in birds adapted to an aquatic lifestyle; in the light of cranial and postcranial aquatic adaptations in *Spinosaurus*, this compactness is interpreted as an additional derived trait. The lower values found in *Suchomimus tenerensis* indicate a more terrestrial lifestyle, as reflected in its osteology.

6. Cranial Semiaquatic Adaptations

Snout Neurovascular Foramina

There are at least 125 neurovascular foramina, which vary in shape, size and density on the referred specimen MSNM V4047. Their density and topographic distribution is very similar to that in living crocodilians. Crocodilian neurovascular foramina that are concentrated on the snout house pressure receptors that are visible to the naked eye as small pigmented protuberances. These protuberances, called "dome pressure receptors" (*44*) or integumentary sensory organs (*16*), lie in the skin over foramina in the underlying

jawbones (*44*) and are very ancient elaborations of trigeminal sensory afferents covering upper and lower jaws. In *S. aegyptiacus* and extant crocodilians, the anterior end of the lower jaw shows a similar concentration of foramina (*1*, *3*). The bony correlates in fossil crocodilians—the concentrated pattern of foramina—look virtually identical to the condition in spinosaurids and *S. aegyptiacus* in particular.

A computed tomographic scan of specimen MSNM V4047 (fig. S6) shows that the snout neurovascular foramina converge deep within the premaxilla and are separate from other spaces within the snout bones, such as alveoli or sinuses (subnarial, nasal, promaxillary). Recent work on extinct marine reptiles such as pliosaurs (*45*) has shown a similar plexus of neurovascular foramina at the anterior end of the snout converging internally to trigeminal afferents.

Research on extant crocodilians (*16*, *44*) has shown that the enhanced sensitivity has diverse functions, such as detection of water movement, feedback for motor response during an initial strike and subsequent bite, and tactile discrimination of prey items held within the jaws. This enhances capture of prey in dark or muddy water or within the mud of a tidal flat. Given the abundance of sawfish, coelacanths, and lungfish in the Kem Kem fauna, we suspect that *S. aegyptiacus* was utilizing a similar sensory system at the surface of the water, underwater, and perhaps within the mud of tidal flats.

Narial Retraction

Witmer (in *6*, p. 892) suggested that the fleshy nostril in *S. aegyptiacus* was located in the anterior portion of a "very subtle narial fossa," which was believed to extend anteriorly from the external naris near the orbital margin along the sidewall of the snout to the subnarial foramen. This is the configuration observed in diplodocoid sauropods, which

have similarly retracted the bony external naris to a location far posteriorly above the orbits. In *Diplodocus*, for example, a subtle fossa is present and can be traced anteroventrally to the subnarial foramen (*46*). Given the evidence for positioning the fleshy nostril toward the anterior end of the narial fossa (*47*), the flesh opening of the naris would remain anterior whereas the bony opening alone has been retracted.

The situation in *S. aegyptiacus*, however, is different (CDS, NI, SM, PCS pers. obs. on referred specimen MSNM V4047). Here there is a clear arcuate and complete narial fossa approximately 10 cm long, directed anteroventrally to the bony opening (Fig. 2C). Both the bony external naris and the surrounding narial fossa are small. There is no further anteroventral extension of the fossa, and so the fleshy nostril must have been small and positioned close to the middle of the skull. This condition appears to be unique among nonavian dinosaurs. The small size and retracted position of the fleshy nostril in *S. aegyptiacus* is a striking semiaquatic adaptation, facilitating breathing at the water-air interface and possibly protecting the fleshy nostrils from struggling prey.

7. Isotopic evidence

Based on the oxygen isotope composition of fossil remains, Amiot *et al*. (*48*) suggested semiaquatic habits in spinosaurids, similar to those of modern day crocodilians and hippopotamuses. Because not all samples provided a clear result (*48*), and because of a lack of body fossils recording adaptations for a semiaquatic lifestyle, these intriguing results could not be evaluated or tested.

8. Stratigraphic Position

The measured section for the Kem Kem sequence was recorded on the south east face of Al Gualb, an isolated 1100 m-tall subconical mesa (Table S5; fig. S7). The base of the section is located at an elevation of 940 m and the top at 1036 m.

The summit of Al Gualb is capped by limestones of the Akrabou Formation, which has yielded a marine invertebrate assemblage including ammonites (*Neolobites*) of late Cenomanian age (~94 Mya). The Kem Kem exposures in the area probably rest on a series of poorly age-constrained conglomerates that outcrop a few kilometers to the south, but the contact is not seen. These, in turn, rest with topographic unconformity on the folded Merdani Formation of Lower Paleozoic age, but the contact is nowhere seen due to an extensive mantle of Quaternary alluvial fans.

Kem Kem exposures between Zrigat in the northeast and Gara Sbaa in the southwest can be divided into two distinct units. The lower of these is dominated by planar bedded, cross bedded and massive, friable sandstones, dominated by pink, brown and yellow brown colors, and a range of grain sizes, but mostly coarse to fine grained. Conglomerates are rare and usually only very thin. The upper unit is dominated by mudstones of varying hues from red, pink, yellow, green and grey. Thin sandstones occur at irregular intervals but are never more than 2 m thick and usually less. Thin limestone occurs in some places, some of which are gastropod coquinas. Gypsum occurs towards the top of the mudstones, but in the region studied beds are rarely more than 1 m thick.

Vertebrate remains occur mainly at concentration horizons of thin conglomerates and grits or as debris flow deposits made of poorly sorted mud-flake rip-up clasts and coarse

sands and grits. These concentration horizons occur mainly in the top third of the lower sandy unit and are found along an outcrop of more than 100 km. Vertebrate remains are rare in the mudstone dominated upper parts of the Kem Kem Formation.

The neotypic skeleton of *S. aegyptiacus* was discovered on the flanks of the plateau immediately to the west of Al Gualb hill (figs. S7, S8). Here the stratigraphy of the lower sand-dominated unit is remarkably similar to that of Al Gualb hill, whereas the mud-dominated upper unit differs in some details. The boundary between the lower sandy unit and the upper mud-dominated unit is transitional, and the partial skeleton occurred within that transition.

We completed the excavation of the specimen, finding and recovering many bone pieces and teeth from the spill pile adjacent to the mouth of the excavation cave (fig. S8). Judging from the number of small pedal bones and the completeness of the hind limbs, we suspect that some articulation of this portion of the skeleton was originally present. We recorded what could be recalled about the positioning of the bones from the local collector who found and excavated the specimen in 2008.

Log Near Zrigat Locality (Table S5)

Latitude/Longitude: The exact locality data can be obtained by request to the corresponding author.

Elevation: 1050 m (by Google Earth), 1100 m from Moroccan map datum. Top of Al Gualb Mesa. 907 m is the lowest point at the base of mesa with *in situ* strata (Fig. S4).

Sheet: Oulad Jallal NH-30-XX-4a, 1st ed. (1984).

Log date: December 1, 2013 (by D. M. Martill).

Section setting: bottom covered; top 3 m covered; 69 beds identified.

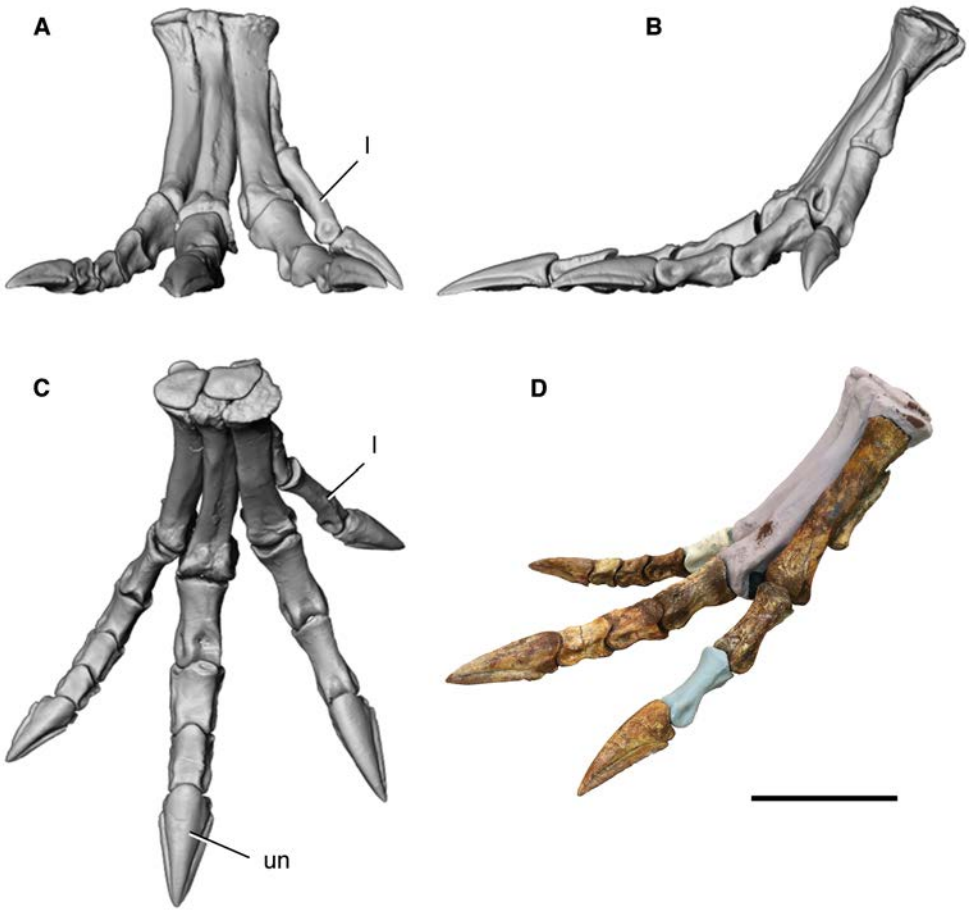

Fig. S1. Reconstructed digital pes of *Spinosaurus.* Foot shown in (**A**) anterior, (**B**) lateral (**C**) dorsal views; (**D**) shows the partially mounted and reconstructed foot of FSAC-KK 11888. Abbreviations: *I*, digit I; *un*, ungual. Scale bar equals 20 cm.

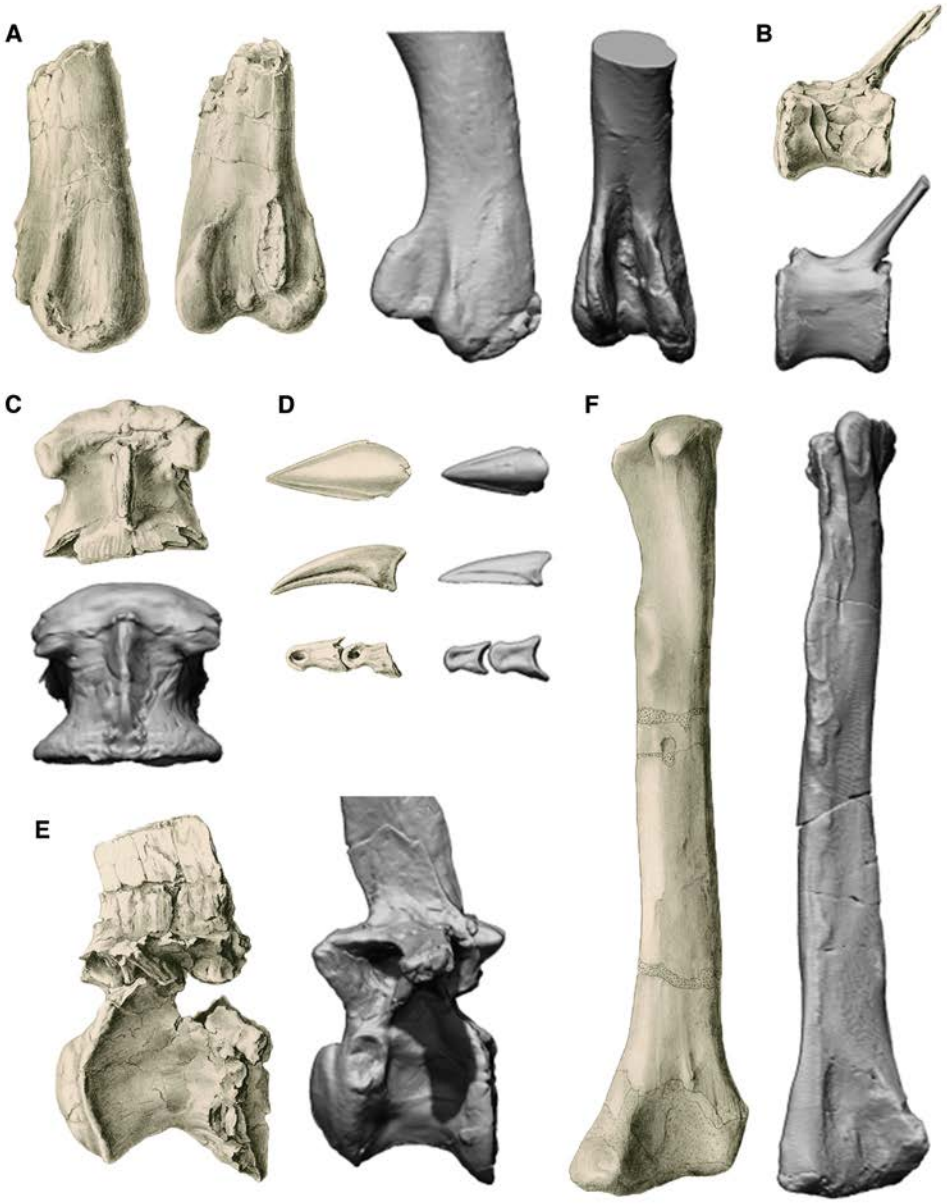

Figure S2. Neotype material (digital elements, in gray) scaled to the same size as material of *Spinosaurus* B (*2*), showing overlap in morphology and proportions. (A) femur, (B) distal caudal, (C) cervicodorsal, (D) pedal ungual and pedal phalanges, (E) dorsal 4 or 5, (F) tibia. Refer to Stromer (1934) for detailed descriptions and scale (*2*). A, D and F are 1:1 comparisons, with the same bones preserved in both associated skeletons.

Note however that the ungual may not be the same digit. The remaining bones are based on reconstructed bones from the digital skeleton.

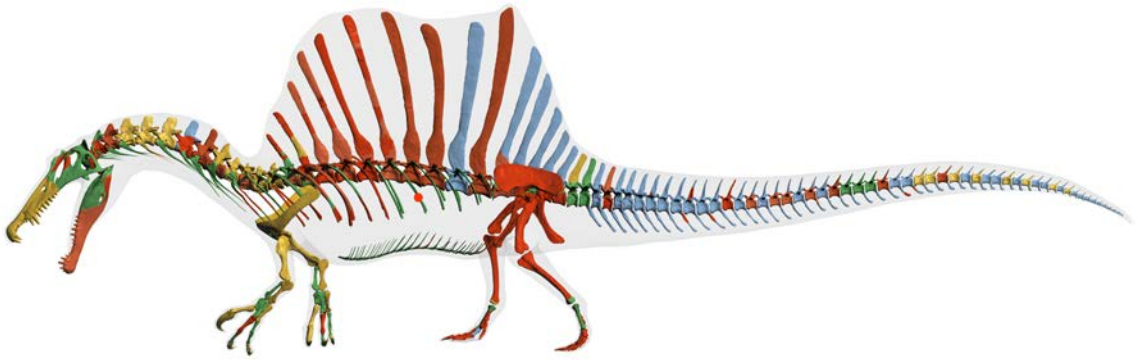

Fig. S3. Digital skeletal reconstruction and transparent flesh outline of *Spinosaurus aegyptiacus*. Color codes are used to show the origin of different parts of the digital skeletal model. Bones of the neotype and for *Suchomimus tenerensis* were CT-scanned, surfaced and size-adjusted before being added to the model. Color coding: ***red***, neotype (FSAC-KK 11888); ***orange***, Stromer's bones; ***yellow***, isolated bones from the Kem Kem; ***green***, surrogate bones modeled or taken from the spinosaurids *Suchomimus*, *Baryonyx*, *Irritator* or *Ichthyovenator*; ***blue***, inferred bones from adjacent bones. A red dot below the posterior dorsal centra shows the approximate position of the center of mass. Model created by Tyler Keillor, with technical assistance of Lauren Conroy and Erin Fitzgerald.

Fig. S4. Skull reconstruction of *Spinosaurus aegyptiacus* showing discovered bones. Skull bones that are known in *S. aegyptiacus* are shown in blue. Artwork by Davide Bonadonna.

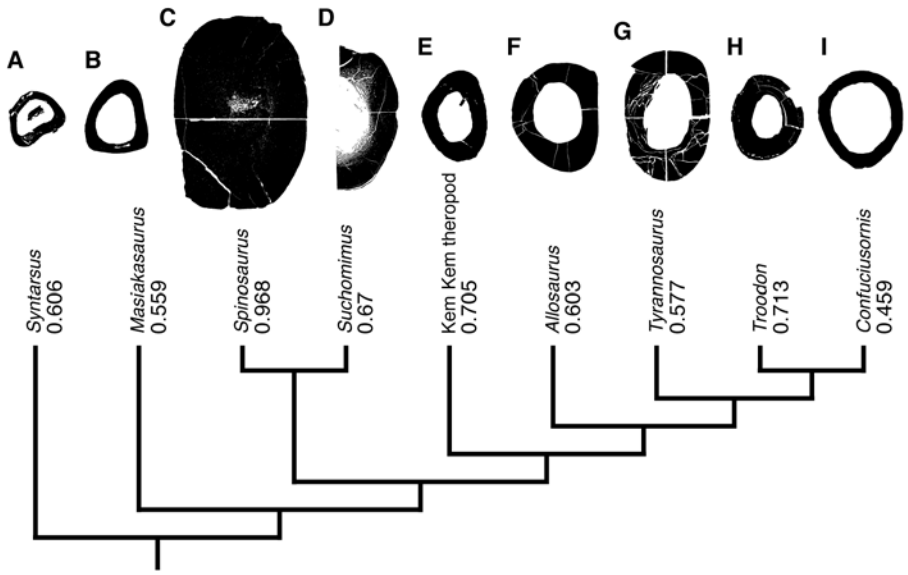

Fig. S5. Bone density among select nonavian theropods and *Confuciusornis*. Bone density calculated from a suite of measures on femoral shaft thin-sections show that *S. aegyptiacus* has by far the most compact bone among nonavian theropods. Values reported on the branches are Global Compactness Values, collected by analysis with Bone Profiler.

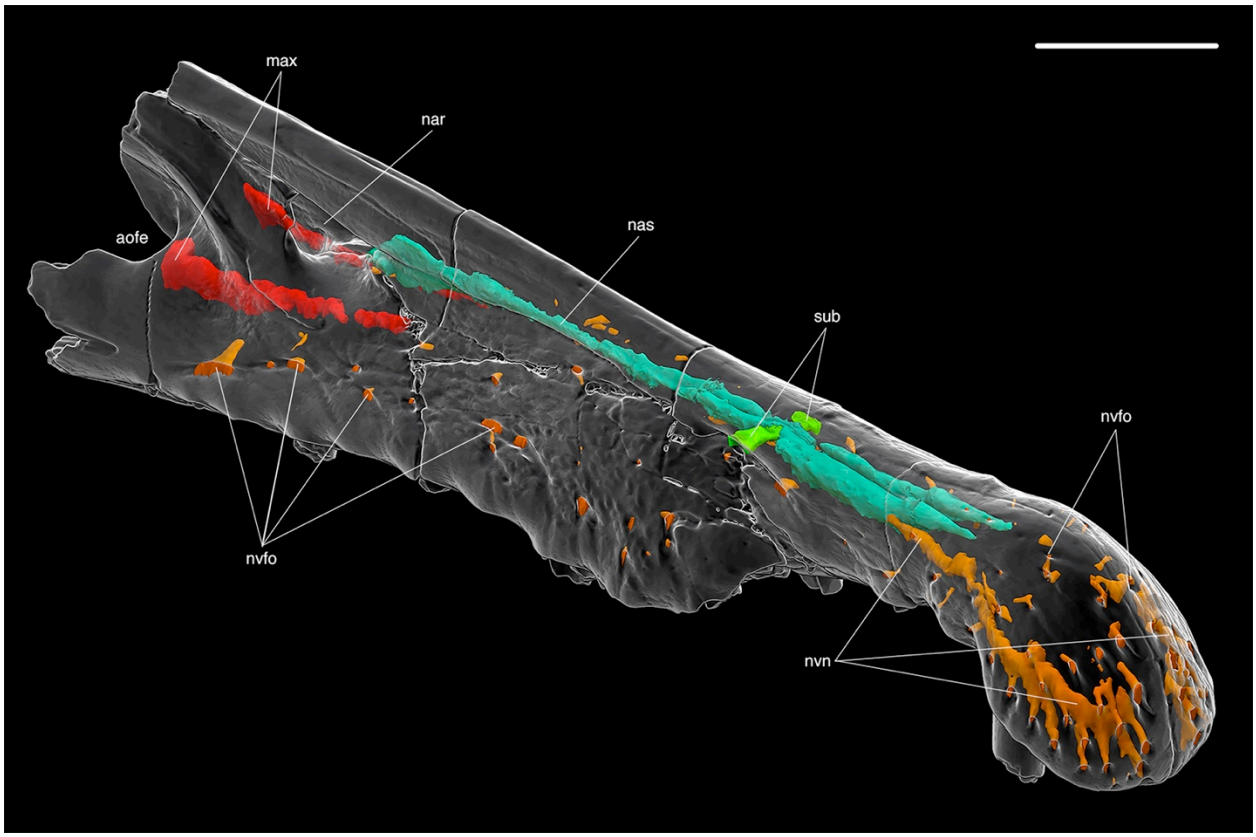

Fig. S6. CT rendering of the adult snout of *Spinosaurus aegyptiacus* (MSNM V4047). Note the neurovascular network (**orange**). The snout scan was taken with a Siemens Somatom Definition Dual Source CT Scanner (Radiology Department, Ospedale Maggiore, Milan) using transverse (axial) slices (scan parameters 120 kV, 120 mA; and slice thickness 0.3 mm.; 2646 slices). Data analysed using OsiriX 5.6 32-bit (http://www.osirix-viewer.com), Mimics 10.01 and ZBrush 4. Matrix filling anatomical cavities was removed digitally. Abbreviations: *aofe*, antorbital fenestra; *max*, promaxillary sinus; *nar*, external naris; *nas*, nasal sinus; *sub*, subnarial sinus and foramen; *nvfo*, neurovascular foramina; *nvn*, neurovascular network. Scale bar equals 10 cm.

Fig. S7. View west from above the site of the neotypic skeleton of *Spinosaurus aegyptiacus*. Several team members stand near the excavation cave that yielded the partial neotypic skeleton (blue arrow). A section was completed on the crest of the excavation. The more complete section given below (Table S5) was completed on the face of an adjacent mesa (yellow arrow).

Fig. S8. View of the excavation cave. The locality is situated in a fluvial sandstone near the base of the upper unit of the Kem Kem sequence. The hammer shaft length marks the position and thickness of the layer that embedded the bones of the neotypic skeleton.

Table S1. Measurements (upper portion) of skull and postcranial bone lengths (in centimeters) and iliac blade area (in square centimeters, square root) and proportions (lower portion, in %) in *Spinosaurus aegyptiacus* and several other large theropods. Measurements are averaged when both sides are available. Parentheses indicate length estimates.

Measure or ratio	***Spinosaurus*** **FSAC-KK 11888**	***Suchomimus*** **MNN GAD500**	***Allosaurus*** **USNM 4734**	***Acrocantho-saurus*** **NCSM 14345**	***Tyrannosaurus*** **FMNH PR 2081**
Body length*	588	600	300	562	600
Skull†	112	120	60	129	140
Humerus	(51)‖	56	31	37	39
Radius	(24)‖	26	22	22	17
Metacarpal II	(23)	(21)	12	12	10
Forelimb+	98	103	65	71	66
Iliac blade area‡ (length, height, area, √area)	70, 30, 2100, 46	100, 53, 5300, 73	70, 31, 2170, 47	(129), (50), 6450, 80	151, 51, 7701, 88
Femur	61	108	85	128	132
Tibia	67	95	69	(96)	114
Metatarsal III	(30)	38	33	(44)	67
Hind limb§	158	241	187	268	313

Forelimb/Body length	17%	17%	22%	13%	11%
√Ilium area/Body length	8%	12%	16%	14%	15%
Hind limb/Body length	27%	40%	62%	48%	52%
Forelimb/Hind limb	62%	43%	35%	27%	21%
Tibia/Femur	110%	88%	81%	75%	86%

[*]Body length is measured along the axial column between the anterior tip of the skull and the posterior extremity of the pelvic girdle.

[†]Skull length measured between the anterior tip of the premaxilla and posterior extremity of the occipital condyle.

[+]Forelimb length equals sum of humerus, radius and metacarpal II.

[‡]Iliac blade area equals maximum blade length times maximum height over the acetabulum.

[§]Hind limb length equals sum of femur, tibia and metatarsal III.

[||]The humerus and radius (not preserved in FSAC-KK 11888) are estimated from comparable bones in the spinosaurid *Suchomimus tenerensis* (MNN GAD500).

Table S2. Skeletal measurements (cm) of the neotype skeleton of *Spinosaurus aegyptiacus* (FSAC-KK 11888). Measurements of paired bones are from the right side except where indicated. Phalangeal length measures the functional chord, from the most invaginated point on the proximal articular socket to the apex of the distal articular condyle or tip of the ungual. Parentheses indicate estimated measurement of complete structure. Abbreviations: *C*, cervical vertebra; *CA*, caudal vertebra; *D*, dorsal vertebra; *S*, sacral vertebra.

Bone	**Measurement (cm)**
Cranium	
Cranium length (premaxilla to quadrate condyle)	(112)
Antorbital fossa maximum length	(30)
Quadrate height	24.0
Axial skeleton	
C2 centrum length	8.0
C7 centrum length	14.5 (15.5)
D6 centrum length	17.0
D7 centrum length	17.0
D8 centrum length	18.0
S3 centrum length	14.5
S4 centrum length	14.0

S5 centrum length	13.5
Chevron 9 length preserved	15.5 (27)
Chevron 11 length preserved	15.5 (25)
Chevron 27 length preserved	9.0 (15)
Forelimb	
Manual phalanx II-1 length	17.5
Pelvic girdle	
Iliac blade length	68.0 (71)
Iliac blade height above acetabulum	18.0
Ilium, width of pubic peduncle, anteroposterior	10.0
Ilium, width of pubic peduncle, mediolateral	4.5
Ischium length	52.0
Ischium, pubic peduncle length	6.0
Ischium, iliac peduncle	9.0
Pubic blade at mid length, transverse width	10.0
Pubic foot length	(12)
Hind limb	
Femur length	61.0
Tibia length	66.8
proximal end, anteroposterior length	16.5
mid shaft, transverse width	7.0
mid shaft, anteroposterior width	4.5
distal end, transverse width	12.0

Fibula length	60.5
distal end, anteroposterior width	4.5
Metatarsal I length	10.5
Pedal phalanx I-1 length	11.5
Pedal phalanx II-1 length	10.0
Pedal phalanx III-1 length	9.0
Pedal phalanx III-2 length	6.5
Pedal phalanx IV-1 length	6.0
Pedal phalanx IV-2 length	5.0
Pedal phalanx IV-3 length	4.0
Pedal phalanx IV-4 length	3.5
Pedal phalanx IV-ungual length	8.0

Table S3. Radial measurements for the femoral thin-section (mm).

Measurement	
Minor axes	29.75
Primary bone exposed	8.28
Broadest zone	2.57
Penultimate zone	1.64
Mean of the last three zones	1.57

Table S4. Radial compactness measurements for the femoral thin-section.

Taxa	Bibliography
Alligator mississippiensis	Lee (2004), http://paleohistology.appspot.com/Page/alligator.html
Aptenodytes patagonicus	Quemeneur *et al*. (2013)
Podiceps cristatus	Quemeneur *et al*. (2013)
Larus ridibundus	Quemeneur *et al*. (2013)
Fulica atra	Quemeneur *et al*. (2013)
Anas platyrhynchos	Quemeneur *et al*. (2013)
Bubulcus ibis	Quemeneur *et al*. (2013)
Apteryx australis	Bourdon *et al*. (2009), fig. 1b
Megapodius nicobariensis	Quemeneur *et al*. (2013)
Casuarius casuarius	Quemeneur *et al*. (2013)
Dromaius novaehollandiae	Quemeneur *et al*. (2013)
Pterocnemia pennata	Quemeneur *et al*. (2013)
Rhea Americana	Quemeneur *et al*. (2013)
Struthio camelus	Quemeneur *et al*. (2013)
Syntarsus sp.	Cortesy by Chinsamy-Turan
Masiakasaurus knopfleri	Lee & O'Connor (2013), http://paleohistology.appspot.com/Page/alligator.html
Suchomimus tenerensis	This study
Spinosaurus aegyptiacus	This study
Unamed theropod from Kem Kem beds	Evans *et al*. (2014), fig. 2
Allosaurus fragilis	Bybee *et al*. (2006), fig. 1
Tyrannosaurus rex	Horner & Padian (2004), fig. 1
Troodon formosus	Varricchio *et al*. (2008), fig. 2
Confuciusornis sanctus	De Ricqlès *et al*. (2003), fig. 2
Accipiter nisus	Quemeneur *et al*. (2013)
Alcedo atthis	Quemeneur *et al*. (2013)
Corvus corone	Quemeneur *et al*. (2013)

Specimen	lifestyle 1	lifestyle 2	lifestyle 3	lifestyle 4	S	P
UCMP 119043	1	0	0	0	0.0324	0.2847

SI	0	0	0	0	0.0461	0.2305
SI	8	3	2	1	0.0138	0.7325
SI	8	3	2	1	0.0109	0.7430
SI	8	3	2	1	0.0182	0.7842
SI	8	3	2	1	0.0173	0.7879
SI	8	3	2	1	0.0180	0.8302
NMW 3606	5	2	2	1	0.0222	0.6474
SI	5	2	2	1	0.0180	0.8153
SI	5	2	2	1	0.0291	0.6635
SI	5	2	2	1	0.0180	0.7848
SI	5	2	2	1	0.0240	0.7099
SI	5	2	2	1	0.0274	0.5657
SI	5	2	2	1	0.0141	0.8740
BPI 753	5	2	2	1	0.0365	0.6681
FMNH 2215	5	2	2	1	0.0167	0.6560
GAD500	5	2	2	1	0.0919	0.5826
FSAC-KK 11888	1	0	0	0	0.0678	0.1989
ROM 65779	5	2	2	1	0.0182	0.5437
UUVP 2656	5	2	2	1	0.0147	0.6113
MOR009	5	2	2	1	0.0370	0.5375
MOR 748	5	2	2	1	0.0563	0.4131
NGMC 98-8-2	7	3	2	1	0.0165	0.7278
SI	7	3	2	1	0.0146	0.8502
SI	7	3	2	1	0.0156	0.7762
SI	7	3	2	1	0.0117	0.7405

Compactness in Center	Compactness at surface	Compactness profile	Global compactness
0.153	0.876	0.723	0.793
0.249	1.004	0.755	0.9541
0	1	1	0.4205
0.001	1.002	1.001	0.4425
0	1.0045	1.0045	0.3495
0.006	0.978	0.972	0.371
-0.002	0.999	1.001	0.3022
0.028	0.95	0.922	0.541
-0.001	1.001	1.002	0.3286
-0.001	0.991	0.992	0.547
0.028	1.01	0.982	0.409
0.001	1.009	1.008	0.4934

-0.001	1.003	1.004	0.6735
0.008	1.012	1.004	0.2475
0.19	0.957	0.767	0.606
0.006	0.99	0.984	0.559
0.193	0.996	0.803	0.67
0.517	0.996	0.479	0.968
0.02	0.998	0.978	0.705
0.059	0.976	0.917	0.603
0.007	0.781	0.774	0.577
0.424	0.913	0.489	0.713
0.092	1.065	0.973	0.459
0	1.0055	1.0055	0.2307
0	1.0035	1.0035	0.3742
0	1.001	1.001	0.4286

Lifestyle 1 0=pelagic; 1=aquatic continental or coastal; 2=amphibious mostly aquatic; 3= amphibious mostly terrestrial; 4=fossorial; 5=terrestrial; 6=arboreal; 7=volant

Lifestyle 2 0=aquatic; 1=amphibious; 2=terrestrial; 3=volant

Lifestyle 3 0=aquatic; 1=amphibious; 2=terrestrial (including volant)

Lifestyle 4 0=aquatic; 1=terrestrial (including volant) or amphibious

Table S5. Stratigraphic log from an excellent exposure on the side of Al Gualb Mesa near the locality of the neotypic specimen.

Bed No.	Thick-ness (m)	Lithology
69	2.00	Grey mudstone
68	1.50	Pink mudstone.
67	0.10	Fine brown sandstone.
66	1.50	Gray mudstone.
65	0.15	Fine sandstone.
64	1.50	Gray mudstone.
63	0.50	Sandstone in two beds.
62	2.50	Gray mudstone with thin sandstone.
61	0.50	Very fine sandstone.
60	2.00	Gray mudstone.
59	0.25	Sandstone, irregularly bedded.
58	5.00	Pink to green mudstone with thin sandstone and purple bands.
57	0.20	Siltstone.
56	1.05	Greenish mudstone.
55	0.30	Thin sandstone interbedded with mudstone.
54	1.00	Pinkish mudstone.

53	0.70	Brown sandstone.
52	0.40	Alternating mudstones and fine sandstone.
51	1.40	Pink mudstone.
50	0.10	band of carbonated nodules.
49	1.40	Mottled pink claystone.
48	0.10	Very fine sandstone.
47	0.04	Mudstone.
46	0.08	Lenticular siltstone.
45	3.00	Pink and gray mudstones.
44	2.50	Purple tinted mudstone.
43	0.25	White mudstone.
42	3.00	Gray mudstone, mottled pink.
41	0.23	Fine brown sandstone.
40	1.00	Red mudstone.
39	1.00	Gray mudstone.
38	1.00	Red mudstone.
37	0.08	Fine brown sandstone.
36	1.50	Red mudstone with thin, interbedded sandstones.
35	1.20	Very fine sandstone.
34	1.00	Mudstone with gypsum.
33	3.00	Green mudstone with interbedded fibrous gypsum.
32	5.00	Gray and pinkish gray mudstone.
31	0.08	Fine laminated gray-colored micrite.

30	0.09	Gray mudstone.
29	0.30	Limestone with gastropods. **first evidence of microinvertebrates**
28	0.60	Pink mudstones.
27	0.30	Green mudstone.
26	1.50	Gray mudstone with thin (0.04 m) bed of fibrous gypsum.
25	0.04	Hard band.
24	0.60	Mottled purple mudstone.
23	0.34	Laminated, domed gypsum with some spherulitic development.
22	0.14	Limestone.
21	0.17	Cream-colored nodular marl. **first hint of carbonate**
20	0.15	Cream-colored mudstone.
19	0.20	Green mudstone.
18	0.13	Red mudstone.
17	0.14	Hard, fine sandy mudstone.
16	1.50	Red-green mottled mudstone.
15	0.05	Purple mudstone.
14	3.00	Red, green mottled mudstone.
13	0.08	Unrecognized lithology (sample taken).
12	0.65	Purple mottled green mudstone.
11	0.09	Greenish anhydrite/gypsum. **first evidence of evaporates**
10	6.00	A more clay rich fine sandstone, which grades from bed 9 below. A mottled horizon is taken as the arbitrary base, which passes up into darker, red-brown mudstones. Weathers back to form slope.

9	12.00	Hard cemented cross bedded medium sandstone with sharp base with flute casts. Basal bedding surface black stained (manganese crust). Some spherulitic concretions. Passes upwards into fine sandstone, but with some coarser, even gritstone layers. Tabular cross-bedded towards top. Some honeycomb weathering. Vertebrate remains include lepidotid scales, sauropod teeth, pterosaur pieces, and fragments of turtle carapace. A circular vertebral centrum may be attributed to the sawfish *Onchopristis*. Some fossil digging by locals. Top of bed ill-defined and passes gradationally into bed 10 above. Supports steep to vertical face.
8	0.60	Green-gray mudstone. Several thin sub-beds can be distinguished in top 15 cm, including 3-4 cm layer of purple-colored ironstone nodules, 3 cm of orange mudstone and 9 cm of green mudstone at very top. Sharp top.
7	2.00	Red mudstone. Gradational boundary with bed 6 below. Grey color of bed below passes into the red of bed 7. Thin iron pan at base. Soft profile.
6	7.00	Soft, gray medium to fine sandstone with some thin (10-20 cm) harder beds. Forms slope rather than vertical surface for first 5 m, but profile steepens at top 2 m.
5	5.00	Massive, fine to medium cross-bedded on 20-40 cm scale buff-colored sandstone with some pinkish layers. Gritty in places with quartz clasts up to 5 mm diameter. Forms vertical outcrops conspicuously dotted with miner bee burrows. Thin iron pan on top of bed.
4	7.00	Cross-bedded with some tabular and massive bedded, pinkish brown, fine sandstone with sharp base and sharp top. Becomes orange/brown for middle 2 m. Includes some yellow/grey lenses. A 2-3 cm grey clay at top is probably a hiatus surface.
3	6.00	Light brown medium sandstone, becomes more red upwards where it passes into light

		green/grey silty clay in top 40-50 cm. Weakly cemented. Some contorted bedding.
2	0.60	Variegated (pink, purple, red, orange, ginger, brown) medium lenticular sandstone. Small bone fragment present. Cross-bedded with some ripple marked surfaces. Current direction 030.
1	5.00	Light brown, ferruginous, weakly cemented, medium sandstone becoming paler and plane-bedded upwards.

References and Notes

1. E. Stromer, *Ahb. König. Bayer. Akad. Wissen. Math-Phys. Kl.* **28**, 1–32 (1915).

2. E. Stromer, *Abh. König. Bayer. Akad. Wissen. Math-Naturwissen. Abt.* **22**, 1–79 (1934).

3. J. B. Smith, M. C. Lamanna, H. Mayr, K. J. Lacovara, New information regarding the holotype of *Spinosaurus aegyptiacus* stromer, 1915. *J. Paleontol.* **80**, 400–406 (2006). doi:10.1666/0022-3360(2006)080[0400:NIRTHO]2.0.CO;2

4. W. Nothdurft, J. Smith, *The Lost Dinosaurs of Egypt* (Random House, NY, 2002).

5. P. Taquet, D. Russell, *C. R. Acad. Sci.* **299**, 347–353 (1998).

6. C. Dal Sasso, S. Maganuco, E. Buffetaut, M. A. Mendez, *J. Vert. Paleont.* **25**, 888–896 (2005). doi:10.1671/0272-4634(2005)025[0888:NIOTSO]2.0.CO;2

7. P. C. Sereno, D. B. Dutheil, M. Iarochene, H. C. E. Larsson, G. H. Lyon, P. M. Magwene, C. A. Sidor, D. J. Varricchio, J. A. Wilson, Predatory dinosaurs from the Sahara and Late Cretaceous faunal differentiation. *Science* **272**, 986–991 (1996). Medline doi:10.1126/science.272.5264.986

8. See the supplementary materials on *Science* Online.

9. R. Lavocat, C. R. Congr, Géol. Int. Paleontol. (1952). *Acad. Sci.* **1**, 65–68 (1954).

10. L. Mahler, Record of Abelisauridae (Dinosauria: Theropoda) from the Cenomanian of Morocco. *J. Vert. Paleont.* **25**, 236–239 (2005). doi:10.1671/0272-4634(2005)025[0236:ROADTF]2.0.CO;2

11. D. A. Russell, *Bull. Mus. Nat. d'Hist. Nat. Paris* **18**, 349–402 (1996).

12. B. McFeeters, M. J. Ryan, S. Hinic-Frlog, C. Schröder-Adams, H. Sues, A reevaluation of *Sigilmassasaurus brevicollis* (Dinosauria) from the Cretaceous of Morocco. *Can. J. Earth Sci.* **50**, 636–649 (2013). doi:10.1139/cjes-2012-0129

13. P. C. Sereno, A. L. Beck, D. B. Dutheil, B. Gado, H. C. E. Larsson, G. H. Lyon, J. D. Marcot, O. W. M. Rauhut, R. W. Sadleir, C. A. Sidor, D. D. Varricchio, G. P. Wilson, J. A. Wilson, A long-snouted predatory dinosaur from Africa and the evolution of spinosaurids. *Science* **282**, 1298–1302 (1998). Medline doi:10.1126/science.282.5392.1298

14. A. J. Charig, A. C. Milner, *Bull. Nat. Hist. Mus* **53**, 11–70 (1997).

15. C. Brochu, *J. Vert. Paleont. Mem. 7*, **22** (suppl. 4), 1–138 (2002).

16. D. B. Leitch, K. C. Catania, Structure, innervation and response properties of integumentary sensory organs in crocodilians. *J. Exp. Biol.* **215**, 4217–4230 (2012). Medline doi:10.1242/jeb.076836

17. F. E. Novas, F. Dalla Vecchia, D. F. Pais, *Rev. Mus. Argent. Cien. Nat.* **7**, 167–175 (2005).

18. F. E. Fish, G. V. Lauder, Passive and active flow control by swimming fishes and mammals. *Annu. Rev. Fluid Mech.* **38**, 193–224 (2006). doi:10.1146/annurev.fluid.38.050304.092201

19. S. I. Madar, *Adv. Vert. Paleobiol* **1**, 353–378 (1998).

20. P. D. Gingerich, Land-to-sea transition in early whales: Evolution of Eocene Archaeoceti (Cetacea) in relation to skeletal proportions and locomotion of living semiaquatic mammals. *Paleobiol* **29**, 429–454 (2003). doi:10.1666/0094-8373(2003)029<0429:LTIEWE>2.0.CO;2

21. F. E. Fish, Structure and mechanics of nonpiscine control surfaces. *IEEE J. Oceanic Eng.* **29**, 605–621 (2004). doi:10.1109/JOE.2004.833213

22. A. Manegold, Two additional synapomorphies of grebes Podicipedidae and flamingos Phoenicopteridae. *Acta Ornithol.* **41**, 79–82 (2006). doi:10.3161/068.041.0113

23. E. Amson, C. de Muizon, M. Laurin, C. Argot, V. de Buffrénil, Gradual adaptation of bone structure to aquatic lifestyle in extinct sloths from Peru. *Proc. Biol. Sci.* **281**, 20140192 (2014). Medline doi:10.1098/rspb.2014.0192

24. K. T. Bates, R. B. J. Benson, P. L. Falkingham, A computational analysis of locomotor anatomy and body mass evolution in Allosauroidea (Dinosauria: Theropoda). *Paleobiol* **38**, 486–507 (2012). doi:10.1666/10004.1

25. S. M. Gatesy, M. Bäker, J. R. Hutchinson, *Paleobiol* **29**, 535–544 (2009).

26. E. Stromer, *Abh. König. Bayer. Akad. Wissen., Math.-Naturwissen. Abt.* **33**, 1–102 (1936).

27. A. J. Charig, A. C. Milner, *Baryonyx*, a remarkable new theropod dinosaur. *Nature* **324**, 359–361 (1986). Medline doi:10.1038/324359a0

28. E. J. Rayfield, A. C. Milner, V. B. Xuan, P. G. Young, Functional morphology of spinosaur ‘crocodile-mimic’ dinosaurs. *J. Vert. Paleont.* **27**, 892–901 (2007). doi:10.1671/0272-4634(2007)27[892:FMOSCD]2.0.CO;2

29. M. L. Casanovas *et al*., *Zub. Monogr.* **5**, 135–163 (1993).

30. J. B. Bailey, *J. Paleontol.* **71**, 1124–1146 (1997).

31. P. Cignoli, M. Corsini, G. Ranzuglia, Meshlab: An open-source 3d mesh processing system. *Ercim news* **73**, 45-46.

32. M. D. Abràmoff, P. J. Magalhães, S. J. Ram, Image processing with ImageJ. *Biophot. Internat.* **11**, 36–43 (2004).

33. A. H. Lee, Histological organization and its relationship to function in the femur of *Alligator mississippiensis*. *J. Anat.* **204**, 197–207 (2004). Medline doi:10.1111/j.0021-8782.2004.00275.x

34. A. S. Quemeneur, V. Buffrénil, M. Laurin, Microanatomy of the amniote femur and inference of lifestyle in limbed vertebrates. *Biol. J. Linn. Soc. Lond.* **3**, 644–655 (2013). doi:10.1111/bij.12066

35. E. Bourdon, J. Castanet, A. de Ricqlès, P. Scofield, A. Tennyson, H. Lamrous, J. Cubo, Bone growth marks reveal protracted growth in New Zealand kiwi (Aves, Apterygidae). *Biol. Lett.* **5**, 639–642 (2009). Medline doi:10.1098/rsbl.2009.0310

36. A. H. Lee, P. M. O'Connor, Bone histology confirms determinate growth and small body size in the noasaurid theropod *Masiakasaurus knopfleri*. *J. Vert. Paleont* **4**, 865–876 (2013). doi:10.1080/02724634.2013.743898

37. D. C. Evans *et al*., Osteology and bone microstructure of new, small theropod dinosaur material from the early Late Cretaceous of Morocco. DOI: 10.1016/j.gr.2014.03.01648.

38. P. J. Bybee, A. H. Lee, E.-T. Lamm, Sizing the Jurassic theropod dinosaur *Allosaurus*: Assessing growth strategy and evolution of ontogenetic scaling of limbs. *J. Morphol.* **267**, 347–359 (2006). Medline doi:10.1002/jmor.10406

39. J. R. Horner, K. Padian, Age and growth dynamics of *Tyrannosaurus rex*. *Proc. Biol. Sci.* **271**, 1875–1880 (2004). Medline doi:10.1098/rspb.2004.2829

40. D. J. Varricchio, J. R. Moore, G. M. Erickson, M. A. Norell, F. D. Jackson, J. J. Borkowski, Avian paternal care had dinosaur origin. *Science* **322**, 1826–1828 (2008). Medline doi:10.1126/science.1163245

41. A. J. de Ricqlès, K. Padian, J. R. Horner, E.-T. Lamm, N. Myhrvold, Osteohistology of *Confuciusornis sanctus* (Theropoda: Aves). *J. Vertebr. Paleontol.* **23**, 373–386 (2003). doi:10.1671/0272-4634(2003)023[0373:OOCSTA]2.0.CO;2

42. P. C. Sereno, F. E. Novas, The skull and neck of the basal theropod *Herrerasaurus ischigualastensis*. *J. Vert. Paleontol.* **13**, 451–476 (1993). doi:10.1080/02724634.1994.10011525

43. R. N. Martínez, P. C. Sereno, O. A. Alcober, C. E. Colombi, P. R. Renne, I. P. Montañez, B. S. Currie, A basal dinosaur from the dawn of the dinosaur era in southwestern Pangaea. *Science* **331**, 206–210 (2011). Medline doi:10.1126/science.1198467

44. D. Soares, Neurology: An ancient sensory organ in crocodilians. *Nature* **417**, 241–242 (2002). Medline doi:10.1038/417241a

45. D. Foffa, A. R. Cuff, J. Sassoon, E. J. Rayfield, M. N. Mavrogordato, M. J. Benton, Functional anatomy and feeding biomechanics of a giant Upper Jurassic pliosaur (Reptilia: Sauropterygia) from Weymouth Bay, Dorset, UK. *J. Anat.* **225**, 209–219 (2014). Medline doi:10.1111/joa.12200

46. J. A. Wilson, P. C. Sereno, Early evolution and higher-level phylogeny of sauropod dinosaurs. *J. Vert. Paleont. Mem.* **7**, 1–68 (1998).

47. L. M. Witmer, Nostril position in dinosaurs and other vertebrates and its significance for nasal function. *Science* **293**, 850–853 (2001). Medline doi:10.1126/science.1062681

48. R. Amiot, E. Buffetaut, C. Lecuyer, X. Wang, L. Boudad, Z. Ding, F. Fourel, S. Hutt, F. Martineau, M. A. Medeiros, J. Mo, L. Simon, V. Suteethorn, S. Sweetman, H.

Tong, F. Zhang, Z. Zhou, Oxygen isotope evidence for semi-aquatic habits among spinosaurid theropods. *Geology* **38**, 139–142 (2010). doi:10.1130/G30402.1